arXiv:2203.11359v1 [quant-ph] 21 Mar 2022

Deploying an inter-European quantum network

Domenico Ribezzo,[1,2] Mujtaba Zahidy,[3] Ilaria Vagniluca,[4] Nicola Biagi,[4] Saverio Francesconi,[1,4] Tommaso Occhipinti,[4] Leif K. Oxenløwe,[3] Martin Lončarić,[5] Ivan Cvitić,[6] Mario Stipčević,[5] Žiga Pušavec,[7] Rainer Kaltenbaek,[7,8] Anton Ramšak,[7] Francesco Cesa,[9] Giorgio Giorgetti,[10] Francesco Scazza,[9,1] Angelo Bassi,[9] Paolo De Natale,[1] Francesco Saverio Cataliotti,[1,11] Massimo Inguscio,[12,1,4] Davide Bacco,[3,4,*] and Alessandro Zavatta[1,4,†]

[1]*Istituto Nazionale di Ottica del Consiglio Nazionale delle Ricerche (CNR-INO), 50125 Firenze, Italy*
[2]*Università degli Studi di Napoli Federico II, Napoli, Italy*
[3]*Center for Silicon Photonics for Optical Communication (SPOC), Department of Photonics Engineering, Technical University of Denmark, Kgs. Lyngby, Denmark*
[4]*QTI S.r.l., 50125, Firenze, Italy*
[5]*Centre of Excellence for Advanced Materials and Sensing Devices, Ruđer Bošković Institute, 10000 Zagreb, Croatia*
[6]*Department of Information and Communication Traffic, Faculty of Transport and Traffic Sciences, University of Zagreb, Croatia*
[7]*University of Ljubljana, Faculty of Mathematics and Physics, 1000 Ljubljana, Slovenia*
[8]*IQOQI - Austrian Academy of Sciences, 1090 Vienna, Austria*
[9]*Department of Physics, University of Trieste, Trieste, Italy*
[10]*ICT service area, University of Trieste, Trieste, Italy*
[11]*Department of Physics, Università degli Studi di Firenze, Firenze, Italy*
[12]*Department of Engineering, Campus Bio-Medico University of Rome, 00128 Rome, Italy*

Around forty years have passed since the first pioneering works have introduced the possibility of using quantum physics to strongly enhance communications safety. Nowadays Quantum Cryptography, and in particular, Quantum Key Distribution (QKD) exited the physics laboratories to become commercial technologies that increasingly trigger the attention of States, military forces, banks, and private corporations. This work takes on the challenge of bringing QKD closer to a consumer technology: optical fibers deployed and used by telecommunication companies of different States have been used to realize a quantum network, the first-ever connecting three different countries. This pushes towards the necessary coexistence of QKD and classical communications on the same infrastructure, which currently represents a main limit of this technology. Our network connects Trieste to Rijeka and Ljubljana via a trusted node in Postojna; a key rate of over 3 kbps has been achieved in the shortest link, and a 7-hour long measurement has demonstrated the system stability and reliability. Finally, the network has been used for a public demonstration of QKD at the G20 Digital Ministers' Meeting in Trieste. The reported experimental results, together with the significant interest that one of the most important events of international politics has attracted, showcase the maturity of the QKD technology bundle, placing it in the spotlight for consumer applications in the near term.

I. INTRODUCTION

The amount of internet traffic is strongly increasing every year, with 5.3 billion internet users expected by 2023 [1]; in the same way, the number of breaches and total records exposed per breach continues to grow as well as the average cost of lost or stolen records [1]. In this scenario, realizing a worldwide quantum network that guarantees strong safety in communications is of utmost importance. Quantum Key Distribution (QKD), proposed by Bennett and Brassard in 1984, is a protocol that can provide unconditionally secure data communications enabled by the laws of quantum physics [2–4]. QKD is the most mature quantum-enabled technology, and multiple Countries have already implemented practical use-cases worldwide. For example, optical fiber links [5–8], satellites [9], or both, have been used to create a quantum network enhancing secure communications among different cities and two different Countries [10]. It is worth noticing that fiber communications over thousands of kilometers are possible only thanks to the trusted-node scenario (quantum states are measured and then subsequently re-encoded) [11–15]. In this way, it is possible to extend the maximum haul of a point-to-point link and to allow connection of multiple users [16]. However, the long-term goal of a unified quantum network across the entire world is hampered by practical difficulties (i.e., different fiber infrastructures, different telecom operators, etc.) of interconnecting more countries through the already existing fibre infrastructure. In this context, one of the goals of the European Quantum Communication Infrastructure (EuroQCI) project [17] is to establish a European quantum network, able to overcome current limitations.

In this work, we kicked-off the EuroQCI initiative by connecting Italy, Slovenia, and Croatia, three different European countries, over an in-fiber quantum network. A BB84 protocol using a time-bin encoding scheme and 1-decoy state method has been used for the different links [18]. The measured key rates in the two links Trieste-Postojna and Ljubljana-Postojna are over 2.0 kbps and 3.1 kbps, respectively, while the key rate in the high-loss link Trieste-Rijeka (25 dB) is 610 bps. The distributed quantum keys have been used to secure a virtual private network (VPN) among the users, which was employed for quantum-secured video-calls during the G20 event held in Trieste.

* dabac@fotonik.dtu.dk
† alessandro.zavatta@ino.cnr.it

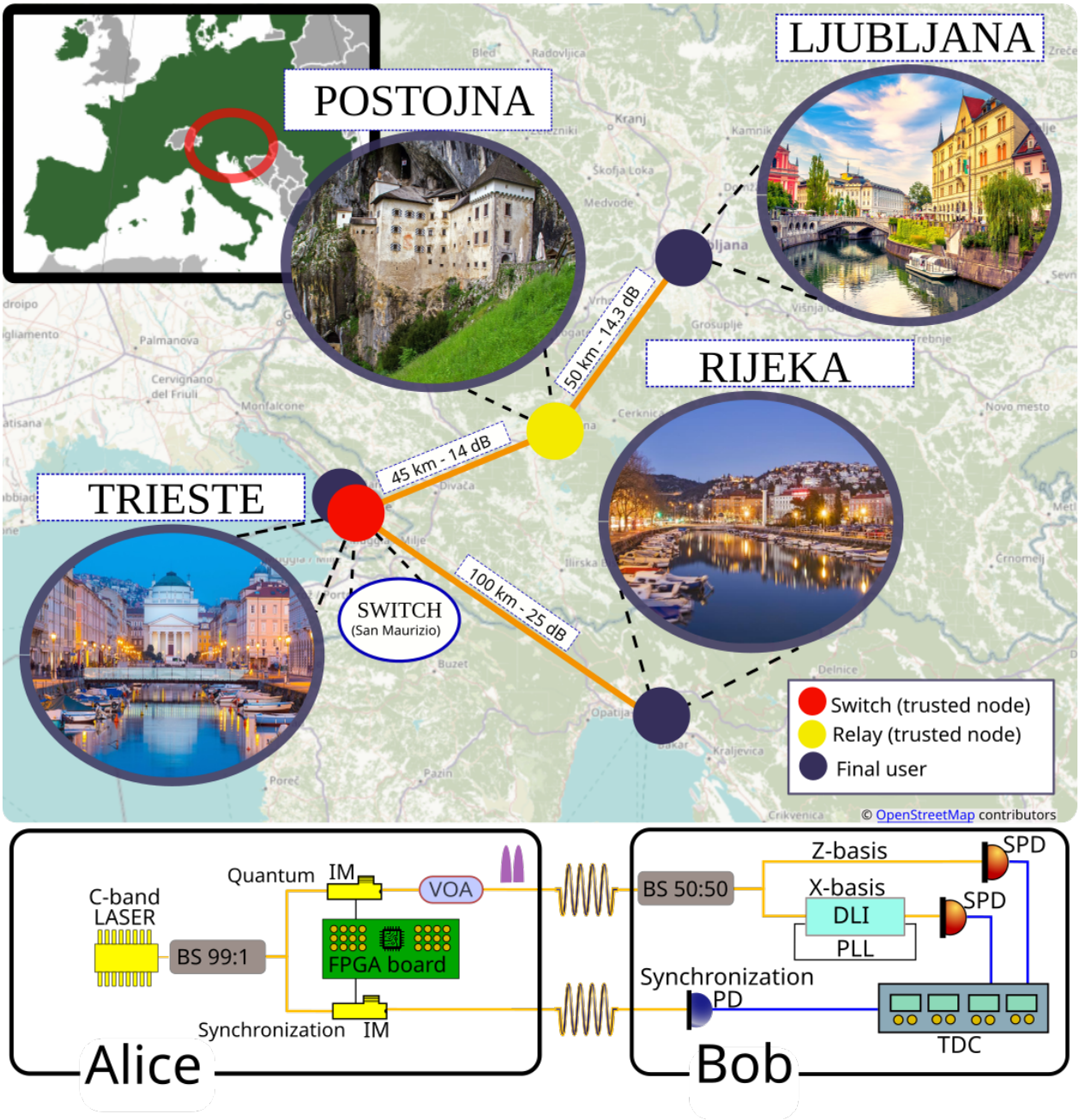


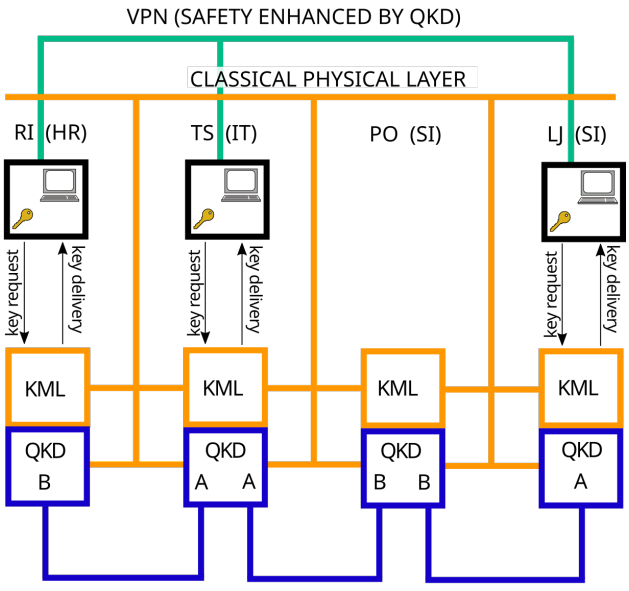
Figure 1. **Network and setup schemes. Top**: The network consists of three links and two trusted nodes. The two transmitters (Alices) are located in Trieste (Italy) and Ljubljana (Slovenia) while there are two receivers (Bobs) in Postojna (Slovenia) and one in Rijeka (Croatia). One transmitter is located in the Trieste Convention Center while a switch acting as a trusted node is located a few kilometers away, in the telecom center of Trieste San Maurizio; this solution renders the San Maurizio center the starting point of the quantum communication channels. The two receivers in Postojna behave as the second trusted node. **Bottom**: On Alice's side, the C-band laser is split by a 99:1 beam splitter (BS 99:1) and is sent to the intensity modulators (IM) controlled by an FPGA board; the 1% output of the beam splitter goes toward the quantum part, while a variable optical attenuation (VOA) is added in order to reach the desired mean photon number per pulse. The 99% BS output is used to generate a low-jitter synchronization signal with a frequency of 145 kHz. On Bob's side, a 50:50 BS is used for the basis choice; for the Z-basis the photons are directly sent to a single photon detector (SPD), while the photons directed to the X-basis detector pass previously through a delay-line interferometer (DLI), whose function is described in the text; in the Trieste-Postojna link, the interferometer is stabilized by a phase lock loop (PLL). The two SPDs, together with a fast photo-diode that reads the synchronization signal (sync PD), are connected to a time-to-digital converter (TDC) that registers the timestamps of events from which, after the post-processing stage, the key is extracted.

II. NETWORK ARCHITECTURE

The implemented network, whose infrastructure is illustrated in Fig. 1 and architecture is reported in Fig. 2, is composed of two transmitters, also called *Alice*, and three receivers, known as *Bob*, connected by two optical fibers; one is used for the quantum signal and the other one is used for the service signal, i.e. synchronization, parameter estimation,



(a) QKD module.



(b) Network architecture.

Figure 2. **a) QKD module.** QKD module mounted in a telecommunication cabinet. **b) Network architecture.** The network works over different levels. The black squares, representing the computers in the meeting rooms, act as both the application layer and the classical logical layer; upon a request to launch the VPN connecting Trieste (TS), Rijeka (RI) and Ljubljana (LJ) nodes. The classical logical layer sends a request to the key management layer (KML), that checks if a ready-to-use key to secure the VPN is already stored. Upon passing this test the key management layer sends the key to the classical logical layer, otherwise, a request to generate a new key is sent to the quantum layer (blue box). The quantum layer is made by the proper optical setup (physical sublayer) and all the post-processing methods necessary to produce the final key (logical sublayer); the A (Alice) or B (Bob) letter in the quantum layer box says if the node is a transmitter or a receiver. When a key is ready, the quantum layer sends it to the key management layer that will deliver it to the first layer. The key management layer, together with the internet infrastructure, make up the classical physical layer.

etc. The first transmitter, located in Trieste Convention Center (TCC), sends the synchronization and the quantum signals encoding the key, towards the telecom center located in Trieste San Maurizio, three kilometers away from TCC. Here, the two signals are divided by two 50:50 beam splitters in order to route them towards two different nodes; this makes San Maurizio the place where the quantum channels start. The two receiving nodes are both located outside the Italian borders, one in the Telekom Slovenije d.d. telecom center in Postojna (Slovenia) and the other one in the OIV telecom center located in Rijeka (Croatia). The Postojna node is not the final user of our network, since it acts as the second trusted node in order to reach the capital city, Ljubljana, a connection not possible with a single direct link since the overall losses were too high (around 30 dB). More specifically, a second Alice was located at the Faculty of Mathematics and Physics of the University of Ljubljana: it worked in a way analogous to the Alice located in Trieste but served just one node. For each link, one dark fiber was used for the quantum channel and a second dark fiber for the synchronization. The communication for the upper layer protocols was established with a standard TCP/IP internet connection. The measured attenuations of the quantum channels were about 14 dB for the links connecting Trieste to Postojna and Ljubljana to Postojna, and 25 dB for the Trieste-Rijeka link. The entire network has been set up in few days, from scratch, using already-deployed fibers from different providers. This quantum network was used to provide a QKD proof-of-principle demonstration at the G20 Digital Ministers' Meeting held in Trieste on August 5^{th}, 2021. Two concerts by the Ljubljana and Rijeka conservatories orchestras were broadcasted to the G20 headquarter in Trieste via videoconference (openmeetings) established over a Virtual Private Network (VPN) reinforced by a quantum key; likewise, the Trieste conservatory orchestra shared a concert with Ljubljana and Rijeka. The quantum network was based on fibers normally used for backup links and regular data traffic, and was hence only available for the amount of time necessary to configure the QKD setups and broadcast the three concerts.

III. QKD SYSTEMS

A. Protocol

The adopted protocol, implemented for all the links, is the three-states efficient BB84 with one decoy method [19–24]. In this scheme, the key is distributed just using the states encoded in the **Z**-basis, while the **X**-basis states are utilized to estimate the amount of information leaked by an eavesdropper. The mean numbers of photons per pulse contained in the signal and decoy states, generally referred to as μ_1 and μ_2, have been chosen in order to maximize the secure key rate, taking into account all the device characteristics. In the finite-key regime the key length l is bound to [19]:

$$l \leq s^l_{Z,0} + s^l_{Z,1}(1 - H_2(\phi^u_Z)) - \lambda_{EC} - 6\log_2\left(\frac{19}{\varepsilon_{sec}}\right) - \log_2\left(\frac{2}{\varepsilon_{corr}}\right), \quad (1)$$

where $s^l_{Z,0}$ and $s^l_{Z,1}$ are the lower bounds for the vacuum and the single-photon events, respectively, ϕ^u_Z is the upper bound of the phase error rate, λ_{EC} is the number of disclosed bits in the error correction stage, $H_2(x) = -x\log_2(x) - (1 -$

$x)\log_2(1-x)$ is the binary entropy and ε_{sec} and ε_{corr} are the secrecy and correctness parameters, defined as [25]:

$$P[S_A \neq S_B] < \varepsilon_{corr},$$
$$\mathbb{1}(S_A, S_B; Z, C) < \varepsilon_{sec},$$

with S_A and S_B being the two sifted keys, $P[x]$ the probability of x, $\mathbb{1}(\cdot)$ a generic information measure, Z is the eavesdropped sequence owned by a potentially malicious part (generally referred to as Eve) and C is a random variable representing the exchanged information. The second term denotes the probability ε_{sec} of having a stronger correlation between Alice's and Eve's strings than Alice's and Bob's one. These parameters have been arbitrarily set as $\varepsilon_{corr} = 10^{-12}$ and $\varepsilon_{sec} = 10^{-9}$. The phase error rate in the **Z**-basis ϕ_Z can generally be estimated from the error rate in the **X**-basis δ_X; however, in the three-state BB84 protocol Alice sends only one quantum state in the **X**-basis, so it cannot be directly measured but it needs to be estimated by the **X**-basis error rate $QBER_X$ as reported in [26]. $QBER_X$ is connected to the visibility vis_X by $QBER_X = (1 - vis_X)/2$.

B. Alice's setup

On Alice's side, a field-programmable gate array (FPGA) is programmed to generate digital signals that drive two intensity modulators, one to prepare the synchronization pulses at a rate of 145.358 kHz via carving a continuous wave (CW) laser, while the other one is producing the time-bin pulses, encoding the quantum states at a rate of around 595 MHz with 800 ps separation between the two bins. The sequence of quantum states is generated according to a pseudo-random binary sequence (PRBS) of length $l = 2^{12} - 1$. The two CW laser beams are derived from the same C-band laser, previously divided by a beam-splitter. Alice's entire setup has been accurately engineered in order to fit in a 2U rack box. Alice makes the basis choice, encoding the qubit into the **Z** (computational) basis with a probability $P_{ZA} = 0.9048$ or choosing the **X** (diagonal) basis with a probability $P_{XA} = 1 - P_{ZA} = 0.0952$. These parameters have also been optimized according to the results of a simulation model, in order to maximize the final secret key rate given the channel loss and the detector efficiencies. It should be noted that, in a real implementation of QKD, the quantum states are required to be phase randomized and the PRBS should be replaced with true random numbers [27].

C. Bob's setup

The qubits received by Bob are randomly measured in **Z** or **X**-basis with equal probability through a 3 dB beam splitter. Concerning the **Z**-basis, measuring the arrival time of the photon is sufficient for decoding the quantum state, while an unbalanced interferometric measurement with a delay line of 800 ps provides the relative phase information, performing the **X**-basis measurement. Two types of interferometers have been used in Bob's setups: a free-space interferometer and a compact all-in-fiber one. The all-in-fiber interferometer is based on a Michelson interferometer with an additional 400 ps delay line in one arm and consists of two Faraday mirrors, a piezo-electric phase shifter, and an adjustable delay line to precisely match the length. The two arms are phase-stabilized with a phase-lock-loop (PLL) that drives the phase shifter according to the feedback provided by monitoring the phase fluctuation of a monitor laser (PLL laser). The PLL laser is mixed with the quantum signal via a dense wavelength division multiplexing device (DWDM) and is sent to the interferometer in a co-propagating way with respect to the quantum signal. A second DWDM separates the quantum signals from the PLL laser, where the latter is monitored with an avalanche photo-diode and provides feedback to the PLL.

The second interferometer [28] is a free-space Mach-Zehnder interferometer, whose arms are again delayed 800 ps with respect to each other. It is equipped with a piezo-electric driven mirror to adjust the phase drifts, however, due to the high stability of the system in the periods of data acquisition, no active stabilization system has been put in place.

Measurements have been performed with single-photon detectors from ID quantique, MPD and Aurea able to provide up to 20% efficiency, and dark counts in the range of 2500 Hz at 20 μs hold-off time. Detection events and their arrival time have then been logged by Qutools QuTAG and Swabian Ultra time-to-digital converters, which both have a temporal resolution of 1 ps and an RMS jitter lower than 10 ps.

IV. RESULTS

Table I summarizes the important parameters and final secret key rates achieved in each link. We began by characterizing the channel loss in each link and proceeded to choose the optimal mean photon numbers that maximize the final secret key rate. The mean photon number for signal (μ_1) and decoy (μ_2) state in Ljubljana-Postojna link has been set to $\mu_1 = 0.15$ and $\mu_2 = 0.06$, while for the source in Trieste, that served two nodes, the mean photon numbers per pulse have been chosen as the best compromise between the two channels.

The average SKR per link obtained is around 2080 bps and 3130 bps for the Trieste-Postojna and the Ljubljana-Postojna link, respectively, while it was found around 610 bps for the longer and high-loss channel of the Trieste-Rijeka link. In all cases, we selected a block size such that the computational time necessary for the post-processing was not longer than the corresponding data acquisition time (*block time*).

Adaptive temporal filters were utilized to compensate for the loss of signal, and for little temporal drift of the pulses due to thermal fluctuations in the fibers as well as to reduce the impact of background noise in measuring the visibility. The systems suffered from ≈ 2.5 kcounts/s dark counts in each basis and the loss of the interferometer introduced by design. Due to the high level of attenuation experienced by the signal in Trieste-Rijeka channel and the low number of counts as a result of that, a 60 ps wide temporal filter was adopted to guarantee a QBER around 5% in the security check basis, while the temporal filters for Trieste-Postojna and Ljubljana-Postojna were set to 100 ps and 200 ps, respectively. The difference is due to different losses in the measurement apparatus, indeed, the Michelson interferometer introduces more losses than the free-space Mach-Zehnder one, thus causing a

lower signal-to-noise ratio in the TS-PO channel.

Figure 3 summarizes the achieved SKRs and long-term stability measurement performed for more than 7 hours. The continuous data acquisition in the Trieste-Postojna channel, which was stabilized with our implemented phase locking system, reflects the performance of the PLL.

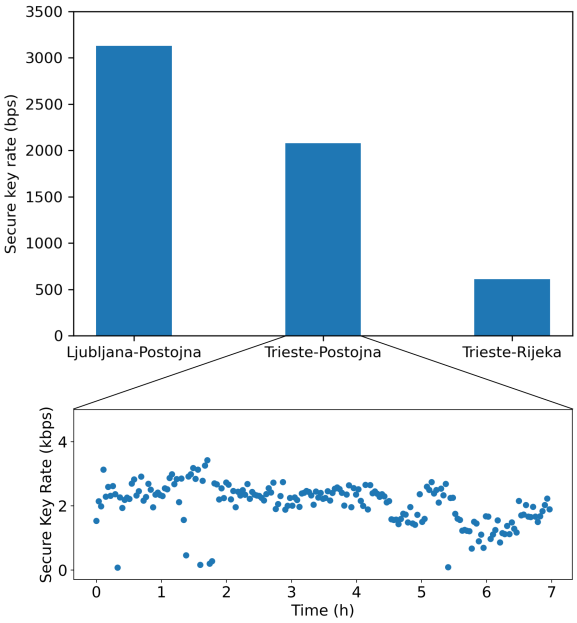


Figure 3. **Secure key rate and stability of the QKD systems.** The graph on top shows the secret key rate in the three links. **Inset graph:** the trend of secure key rate in the Trieste-Postojna link for a duration of approximately 7 hours; each point represents 130 seconds of data acquisition, corresponding to the chosen block size.

	TS-PO	LJ-PO	TS-RI
Attenuation (dB)	14	14.3	25
μ_1	0.24	0.15	0.24
μ_2	0.11	0.06	0.11
Block size n_Z	$1.8 \cdot 10^6$	$1.2 \cdot 10^6$	$6.0 \cdot 10^6$
Block time (min)	2.2	1.0	32.6
$\mathrm{QBER}_Z(\%)$	1.29	0.82	2.90
$\mathrm{QBER}_X(\%)$	5.2	7.0	5.15
SKR(bps)	2080	3130	610
Temporal Filters (ps)	100	200	60
Loss_Z(dB)	1.4	0.2	0.8
Loss_X(dB)	8.6	5.2	1.5

Table I. Specifications of the network and experimental measurements on the three links Trieste-Postojna (TS-PO), Trieste-Ljubljana (TS-LJ) and Trieste-Rijeka (TS-RJ). The data are explained in the text.

V. DISCUSSION AND CONCLUSIONS

This work represents the first step towards the EuroQCI [17]. So far, several countries around the world have already established QKD networks which are up and running and are implemented for various use-cases. e.g., banks, governments, medical centers, etc. In a similar way, Europe is focusing on the development of a European quantum communication network that faces several challenges: multiple vendors, different standards, various implementations of QKD protocols, and "classical" infrastructures. This work represents a concrete step towards the realization of such networks, considering that three QKD systems based on the same protocol but realized by different partners (QTI s.r.l., CNR-INO, DTU) have been combined together distributing a quantum key. Despite the fact that the implemented QKD protocol was the same for all the systems, different measurement apparatuses have been adopted in each receiver taking into account the peculiarities of each link. In particular, the Trieste-Rijeka link employed an ultra-low-loss free-space interferometer to partially compensate for the high channel attenuation. Notwithstanding this loss, as high as 25 dB, it was possible to realize a stable QKD link, which is quite difficult to achieve using standard InGaAs detectors. The reason for the lower key rate in the Trieste-Postojna link, with respect to the Ljubljana-Postojna one with similar attenuation (14 dB), is due to the fact that the second link shows a 1.2 dB lower attenuation in the **Z**-basis, which cannot be fully compensated by the lower **X**-basis QBER.

It is important to note that the fiber network that we have used has been temporarily established for this specific purpose and this has been possible thanks to the cooperation of the Italian, Slovenian, and Croatian telecommunication operators. In this context, it is crucial to remark that some of the devices we have employed in our demonstration are not optimized for application to a real telecom-grade QKD system. Possible improvements include a real-time optical switch, which should be preferred for nodes where a transmitter serves more than one user instead of our beam-splitter, and a real-time quantum random number generator (QRNG), which should be used in all Alice's devices.

Finally, we would like to stress two facts. First, although a generic network should connect any two users (and not the only adjacent ones), the configuration we have adopted allows to share the paired keys between two parties using a trusted-node strategy. For example, Rijeka and Ljubljana, even though not directly connected, can share a key by XORing the keys generated between Trieste-Rijeka, Trieste-Postojna and Postojna-Ljubljana. Second, there is no practical difference between a trusted node made of a switch and a node made of two receiver modules: different nodes produce different keys even if they share the same transmitter since it is the peculiarity of the link (e.g. losses, detector efficiencies, etc.) that generates the exact key.

In conclusion, we have demonstrated an inter-European QKD network during the G20 event held in Trieste. Employing two trusted nodes, we have successfully managed to distribute quantum keys among three different users and to secure a virtual private network among all of them using these keys. This work paves the way towards a fully-fledged European quantum network with concrete use-cases.

VI. METHODS

To extract a final error-free secret key with guaranteed security, post-processing of the raw time tags registered by Bob is necessary. Post-processing comprises a series of steps explained in detail below.

A. Sifting

Alice and Bob start the post-processing by sifting the instances of preparation-measurement that match with each other and discarding the rest. At this stage, Bob communicates the time and the basis in which a measurement is registered via the classical physical layer. Note that only the basis chosen by Bob is communicated and not the measurement result in that basis. Alice returns the list of detection events which Bob measured in the correct basis as well as selected μ of those instances and they discard the rest. Furthermore, Alice discards instances that are not registered due to loss in the channel. The sifted key, however, may contain errors and correlations with Eve.

The size of the sifted key block for each link has been chosen as the largest one such that the post-processing time is not longer than the acquisition time.

B. Error correction

A reconciliation process is necessary to guarantee that Alice and Bob shared the same key. We employed a cascade algorithm [29, 30] to remove any errors in the keys that could have been caused by imperfect measurement, noise, or eavesdropper. According to the cascade algorithm, the shared sifted key is split into blocks whose parities are compared and, when a mismatch is found, a dichotomic search is performed in order to identify and correct the mismatching bits. A series of iterations with block sizes progressively doubled has guaranteed the total accordance between the two keys. An initial block size of $k_1\lceil 0.73/QBER\rceil$ has been chosen as proposed in [30], while a number $n = 8$ of iterations has been chosen in order to drastically minimize the failure probability. Although these choices produce a bigger bit leakage than other proposals [31, 32], they have been preferred in order to minimize the failure probability of this post-processing step [33]. A measure of the efficiency of an error correction algorithm is the error reconciliation efficiency f_{EC}, defined as [33]:

$$f_{EC} = \frac{1 - m/n_Z}{H_2(\varepsilon)},$$

where m is the length of the message exchanged for the reconciling procedure, n_Z is the block size and ε is the quantum bit error rate. The error reconciliation efficiencies for the three links are reported in table II.

Link	f_{EC}
Trieste-Postojna	1.28
Trieste-Rijeka	1.26
Ljubljana-Postojna	1.25

Table II. Error reconciliation efficiency f_{EC} for each link.

C. Error verification

The purpose of error-correction is to remove any discrepancies between Alice's and Bob's strings and, hence, it is necessary to verify its success. In order to compare the strings without disclosing it entirely, Alice and Bob calculate the hash value of their error-corrected sifted key and communicates it to each other to check their agreement.

With the desired $\varepsilon_{corr} = 10^{-12}$, this causes further 40 bits to be discarded in the next privacy amplification step, since $log_2\lceil 1/\varepsilon_{corr}\rceil = 40$ [25].

D. Privacy amplification

Upon a positive outcome from error verification step, Alice and Bob share an identical key with error probability ε_{corr}. Nevertheless, partial information may be leaked to Eve. *Privacy amplification* (PA) is necessary to minimize Eve's correlation with the sifted and error-corrected key, hence, leaving Alice and Bob with a shared information-theoretic secure key.

PA is achieved by applying a universal hash function in the form of a binary Toeplitz matrix. To form the Toeplitz matrix, Alice generates a string of $n_Z + l - 1$ bits and sends it to Bob, where n_Z is the block size and l the final key length, as defined in Eq. (1) [34]. A $l \times n_Z$ Toeplitz matrix T is built on both sides using the bit string, and finally the dot product $T \cdot key_{sifted}$ produces the privacy-amplified-key. The algorithm has been made less costly in terms of usage of memory and execution time by avoiding to build the matrix all at once [35] while adopting parallel executions of the loops.

E. Secure VPN

The final information-theoretic secure keys, generated by QKD, are ready to be used in crypto devices to encrypt data via standard encryption protocols, such as One Time Pad (OTP) or Advanced Encryption Standard (AES-256). In this experiment, instead of using commercial crypto devices, the keys were used to establish an end-to-end encryption (E2EE) via a virtual private network (VPN), a technology able to establish a private network over the public internet network. Whit this method, the certificate required by the VPN is securely communicated between the parties. An E2EE communication is resilient to eavesdropping as long as the key is undisclosed.

In this work, a Secure VPN based on OpenVPN software [36] has been established among all the nodes and its security has been enhanced by QKD by adding a level of security above and beyond that provided by standard SSL/TLS protocols. Since our VPN used 2048 bit-sized keys, Alice and

Bob split their privacy-amplified-keys in blocks of 2048 bits, representing the final keys.

VII. ACKNOWLEDGEMENTS

This work was partially supported by the NATO Science for Peace and Security program (Grant No. G5485, project SEQUEL), the European Union - PON Ricerca e Innovazione 2014-2020 FESR (Grant no. ARS01_00734, project QUANCOM), the Center of Excellence SPOC - Silicon Photonics for Optical Communications (ref DNRF123), the Innovationsfonden (No. 9090-00031B, FIRE-Q) the EraNET Cofund Initiatives QuantERA within the European Union's Horizon 2020 research and innovation program (grant agreement No. 731473, project SQUARE), the Region Friuli Venezia Giulia (project "Quantum FVG"), the H2020 FET Project TEQ (Grant No. 766900), the Croatian Science Foundation HRZZ (grant No. IPS- 2020-1-2616) and the Croatian Ministry of Science and Education MSE (grant No. KK.01.1.1.01.0001). A.R. acknowledges ARRS (grant J2-2514). R.K. and Ž.P. acknowledge support by the Slovenian Research Agency (research projects N1-0180, J2-2514, J1-9145 and P1-0125). The authors acknowledge, the Italian Ministry for Economic Development (MISE) and the Italian Ministry for Foreign Affairs and International Cooperation (MEACI) for hosting the demonstration during the G20 and for the logistic support, and the Ministry of Foreign and European Affairs of the Republic of Croatia.

The authors acknowledge Tommaso Calarco for his valuable support, TIM S.p.A., Telecom Italia Sparkle S.p.A., Telekom Slovenije d.d., Stelkom and Odašiljači i veze d.o.o. (OIV) for making possible all the experiments, providing optical (dark) fiber infrastructure and great technical support.

The authors acknowledge LightNet, the optical-fiber infrastructure of the research and academic centers of the Region Friuli Venezia Giulia, in particular Prof. Antonio Lanza, for providing the local fiber connections and for the technical support.

[1] Cisco. Cisco annual internet report - white paper, 2018. https://www.cisco.com/c/en/us/solutions/collateral/executive-perspectives/annual-internet-report/white-paper-c11-741490.pdf.

[2] Charles H Bennett and Gilles Brassard. Quantum cryptography: public-key distribution and coin tossing. In Proceedings of IEEE International Conference on Computers Systems and Signal Processing, pages 175–179, 1984.

[3] Valerio Scarani, Helle Bechmann-Pasquinucci, Nicolas J Cerf, Miloslav Dušek, Norbert Lütkenhaus, and Momtchil Peev. The security of practical quantum key distribution. Reviews of modern physics, 81(3):1301, 2009.

[4] Eleni Diamanti, Hoi-Kwong Lo, Bing Qi, and Zhiliang Yuan. Practical challenges in quantum key distribution. npj Quantum Information, 2:16025, 2016.

[5] Yu-Ao Chen, Qiang Zhang, Teng-Yun Chen, Wen-Qi Cai, Sheng-Kai Liao, Jun Zhang, Kai Chen, Juan Yin, Ji-Gang Ren, Zhu Chen, and et al. An integrated space-to-ground quantum communication network over 4,600 kilometres. Nature, 589(7841):214–219, 2021.

[6] J. F. Dynes, A. Wonfor, W. W. Tam, A. W. Sharpe, R. Takahashi, M. Lucamarini, A. Plews, Z. L. Yuan, A. R. Dixon, J. Cho, and et al. Cambridge quantum network. npj Quantum Information, 5(1), 2019.

[7] Sören Wengerowsky, Siddarth Koduru Joshi, Fabian Steinlechner, Julien R. Zichi, Sergiy M. Dobrovolskiy, René van der Molen, Johannes W. N. Los, Val Zwiller, Marijn A. M. Versteegh, Alberto Mura, Davide Calonico, Massimo Inguscio, Hannes Hübel, Liu Bo, Thomas Scheidl, Anton Zeilinger, André Xuereb, and Rupert Ursin. Entanglement distribution over a 96-km-long submarine optical fiber. Proceedings of the National Academy of Sciences, 116(14):6684–6688, 2019.

[8] Siddarth Koduru Joshi, Djeylan Aktas, Sören Wengerowsky, Martin Lončarić, Sebastian Philipp Neumann, Bo Liu, Thomas Scheidl, Guillermo Currás Lorenzo, Željko Samec, Laurent Kling, et al. A trusted node–free eight-user metropolitan quantum communication network. Science advances, 6(36):eaba0959, 2020.

[9] Juan Yin, Yu-Huai Li, Sheng-Kai Liao, Meng Yang, Yuan Cao, Liang Zhang, Ji-Gang Ren, Wen-Qi Cai, Wei-Yue Liu, Shuang-Lin Li, and et al. Entanglement-based secure quantum cryptography over 1,120 kilometres. Nature, 582(7813):501–505, 2020.

[10] Sheng-Kai Liao, Wen-Qi Cai, Johannes Handsteiner, Bo Liu, Juan Yin, Liang Zhang, Dominik Rauch, Matthias Fink, Ji-Gang Ren, Wei-Yue Liu, Yang Li, Qi Shen, Yuan Cao, Feng-Zhi Li, Jian-Feng Wang, Yong-Mei Huang, Lei Deng, Tao Xi, Lu Ma, Tai Hu, Li Li, Nai-Le Liu, Franz Koidl, Peiyuan Wang, Yu-Ao Chen, Xiang-Bin Wang, Michael Steindorfer, Georg Kirchner, Chao-Yang Lu, Rong Shu, Rupert Ursin, Thomas Scheidl, Cheng-Zhi Peng, Jian-Yu Wang, Anton Zeilinger, and Jian-Wei Pan. Satellite-relayed intercontinental quantum network. Phys. Rev. Lett., 120:030501, Jan 2018.

[11] Sebastian Philipp Neumann, Domenico Ribezzo, Martin Bohmann, and Rupert Ursin. Experimentally optimizing qkd rates via nonlocal dispersion compensation. Quantum Science and Technology, 6(2):025017, 2021.

[12] Davide Bacco, Ilaria Vagniluca, Daniele Cozzolino, Søren MM Friis, Lasse Høgstedt, Andrea Giudice, Davide Calonico, Francesco Saverio Cataliotti, Karsten Rottwitt, and Alessandro Zavatta. Toward fully-fledged quantum and classical communication over deployed fiber with up-conversion module. Advanced Quantum Technologies, 4(7):2000156, 2021.

[13] Qiang Zhang, Hiroki Takesue, Toshimori Honjo, Kai Wen, Toru Hirohata, Motohiro Suyama, Yoshihiro Takiguchi, Hidehiko Kamada, Yasuhiro Tokura, Osamu Tadanaga, et al. Megabits secure key rate quantum key distribution. New Journal of Physics, 11(4):045010, 2009.

[14] Jiu-Peng Chen, Chi Zhang, Yang Liu, Cong Jiang, Weijun Zhang, Xiao-Long Hu, Jian-Yu Guan, Zong-Wen Yu, Hai Xu, Jin Lin, et al. Sending-or-not-sending with independent lasers: Secure twin-field quantum key distribution over 509 km. Physical review letters, 124(7):070501, 2020.

[15] Hui Liu, Cong Jiang, Hao-Tao Zhu, Mi Zou, Zong-Wen Yu, Xiao-Long Hu, Hai Xu, Shizhao Ma, Zhiyong Han, Jiu-Peng Chen, et al. Field test of twin-field quantum key distribution through sending-or-not-sending over 428 km. Physical Review Letters, 126(25):250502, 2021.

[16] Tom Vergoossen, Sergio Loarte, Robert Bedington, Hans Kuiper, and Alexander Ling. Modelling of satellite constel-

lations for trusted node qkd networks. Acta Astronautica, 173:164–171, 2020.

[17] EuroQCI. European quantum communication infrastructure (euroqci) initiative, 2017. https://digital-strategy.ec.europa.eu/en/policies/european-quantum-communication-infrastructure-euroqci.

[18] Davide Bacco, Beatrice Da Lio, Daniele Cozzolino, Francesco Da Ros, Xueshi Guo, Yunhong Ding, Yusuke Sasaki, Kazuhiko Aikawa, Shigehito Miki, Hirotaka Terai, Hirotaka Terai, Taro Yashimita, Jonas S. Neergaard-Nielsen, Michael Galili, Karsten Rottwitt, Ulirk A. Andersen, Toshio Morioka, and Leif K. Oxenløwe. Boosting the secret key rate in a shared quantum and classical fibre communication system. Communications Physics, 2(1):1–8, 2019.

[19] Alberto Boaron, Gianluca Boso, Davide Rusca, Cédric Vulliez, Claire Autebert, Misael Caloz, Matthieu Perrenoud, Gaëtan Gras, Félix Bussières, Ming-Jun Li, Daniel Nolan, Anthony Martin, and Hugo Zbinden. Secure quantum key distribution over 421 km of optical fiber. Phys. Rev. Lett., 121:190502, Nov 2018.

[20] S. N. Molotkov and S. S. Nazin. Quantum cryptography based on the energy-time uncertainty relation. Journal of Experimental and Theoretical Physics Letters, 63(11):924–929, 1996.

[21] B-S Shi, Y-K Jiang, and G-C Guo. Quantum key distribution using different-frequency photons. Applied Physics B, 70(3):415–417, 2000.

[22] Chi-Hang Fred Fung and Hoi-Kwong Lo. Security proof of a three-state quantum-key-distribution protocol without rotational symmetry. Physical Review A, 74(4):042342, 2006.

[23] Davide Rusca, Alberto Boaron, Marcos Curty, Anthony Martin, and Hugo Zbinden. Security proof for a simplified Bennett-Brassard 1984 quantum-key-distribution protocol. Physical Review A, 98(5):052336, 2018.

[24] Davide Rusca, Alberto Boaron, Fadri Grünenfelder, Anthony Martin, and Hugo Zbinden. Finite-key analysis for the 1-decoy state QKD protocol. Applied Physics Letters, 112(17):171104, 2018.

[25] Matteo Canale. Classical processing algorithms for Quantum Information Security. PhD thesis, Department of Information Engineering, University of Padova, 2014.

[26] Alberto Boaron, Boris Korzh, Raphael Houlmann, Gianluca Boso, Charles Ci Wen Lim, Anthony Martin, and Hugo Zbinden. Detector-device-independent quantum key distribution: Security analysis and fast implementation. Journal of Applied Physics, 120(6):063101, 2016.

[27] Mujtaba Zahidy, Hamid Tebyanian, Daniele Cozzolino, Yaoxin Liu, Yunhong Ding, Toshio Morioka, Leif K. Oxenløwe, and Davide Bacco. Quantum randomness generation via orbital angular momentum modes crosstalk in a ring-core fiber. AVS Quantum Science, 4(1):011402, 2022.

[28] Bacco, Davide, Vagniluca, Ilaria, Da Lio, Beatrice, Biagi, Nicola, Della Frera, Adriano, Calonico, Davide, Toninelli, Costanza, Cataliotti, Francesco S., Bellini, Marco, Oxenløwe, Leif K., and Zavatta, Alessandro. Field trial of a three-state quantum key distribution scheme in the florence metropolitan area. EPJ Quantum Technol., 6(1):5, 2019.

[29] Charles H Bennett, François Bessette, Gilles Brassard, Louis Salvail, and John Smolin. Experimental quantum cryptography. Journal of cryptology, 5(1):3–28, 1992.

[30] Gilles Brassard and Louis Salvail. Secret-key reconciliation by public discussion. In Workshop on the Theory and Application of of Cryptographic Techniques, pages 410–423. Springer, 1993.

[31] M. van Dijk and A. Koppelaar. High rate reconciliation. In Proceedings of IEEE International Symposium on Information Theory, pages 92–, 1997.

[32] Hao Yan, Tienan Ren, Xiang Peng, Xiaxiang Lin, Wei Jiang, Tian Liu, and Hong Guo. Information reconciliation protocol in quantum key distribution system. In 2008 Fourth International Conference on Natural Computation, volume 3, pages 637–641, 2008.

[33] Jesus Martinez-Mateo, Christoph Pacher, Momtchil Peev, Alex Ciurana, and Vicente Martin. Demystifying the information reconciliation protocol cascade. arXiv preprint arXiv:1407.3257, 2014.

[34] Evgeny Kiktenko, Anton Trushechkin, Yury Kurochkin, and Aleksey Fedorov. Post-processing procedure for industrial quantum key distribution systems. Journal of Physics: Conference Series, 741:012081, aug 2016.

[35] Bang-Ying Tang, Bo Liu, Yong-Ping Zhai, Chun-Qing Wu, and Wan-Rong Yu. High-speed and large-scale privacy amplification scheme for quantum key distribution. Scientific reports, 9(1):1–8, 2019.

[36] OpenVPN. Openvpn open source, 2022. https://openvpn.net/community-resources/.